As per UGC guidelines an electronic bar code is provided to secure your paper

International Journal for Modern Trends in Science and Technology
Volume 12, Issue 07, pages 219-231.
ISSN: 2455-3778 online
Available online at: http://www.ijmtst.com/vol12issue06.html
DOI: https://doi.org/10.5281/zenodo.21535124

Design and Performance Analysis of a Fuzzy Logic Controlled BLDC Motor Drive for Integrated Electric Vehicle Charging Applications

M. Bhanu Prakash | N. Susmith | Dr. K. Siva Kumar

Department of Electrical & Electronics Engineering, Sri Venkatesa Perumal College of Engineering and Technology, Puttur, Andhra Pradesh, India.

To Cite this Article
M. Bhanu Prakash, N. Susmith & Dr. K. Siva Kumar (2026). Design and Performance Analysis of a Fuzzy Logic Controlled BLDC Motor Drive for Integrated Electric Vehicle Charging Applications. International Journal for Modern Trends in Science and Technology, 12(07), 219-231. https://doi.org/10.5281/zenodo.21535124

Article Info
Received: 18 June 2026; Revised: 18 July 2026; Accepted: 23 July 2026.

KEYWORDS

Brushless DC (BLDC) motor, Electric vehicle (EV), Fuzzy Logic Controller (FLC), Proportional–Integral (PI) controller, Bridgeless boost PFC converter, Totem-pole converter, Bidirectional DC–DC converter, Integrated EV charging.

ABSTRACT

This paper presents the design and performance analysis of a Fuzzy Logic Controller (FLC)-based Brushless DC (BLDC) motor drive for an integrated electric vehicle (EV) charging and propulsion system. The proposed system combines battery charging and vehicle driving operations using a common DC-link architecture to improve power density, reduce hardware complexity, and enhance overall system efficiency. During the charging operation, a bridgeless boost power factor correction (PFC) totem-pole converter is employed to convert the single-phase AC supply into a regulated DC output with near-unity power factor, low total harmonic distortion (THD), and high conversion efficiency. A bidirectional DC–DC buck–boost converter regulates the battery charging current and maintains a stable DC-link voltage under constant-current charging conditions. During the EV driving operation, the bidirectional DC–DC converter supplies the regulated DC-link voltage to dual three-phase voltage source inverters, which drive the BLDC motors for vehicle propulsion. A Fuzzy Logic Controller is implemented for motor speed control using the speed error and change in speed error as input variables. The performance of the proposed FLC is compared with that of a conventional Proportional–Integral (PI) controller under reference speed changes and load disturbances. Simulation results obtained using MATLAB/Simulink demonstrate that the proposed FLC achieves faster dynamic response, superior speed tracking, lower steady-state error, reduced electromagnetic torque ripple, and improved disturbance rejection compared with the PI controller. Furthermore, the proposed charging system provides efficient battery charging with improved input power quality, stable DC-link voltage regulation, and high conversion efficiency. These results demonstrate that the proposed integrated charging and propulsion architecture provides a compact, reliable, and high-performance solution for next-generation electric vehicle

1. INTRODUCTION

The transportation business has been revolutionized as a result of the fast development of electric vehicles (EVs), which provide an alternative to traditional cars powered by internal combustion engines that is more ecologically friendly. Increasing worries about emissions of greenhouse gases, the depletion of resources for fossil fuels, and tough environmental laws have all contributed to the acceleration of the adoption of electric vehicles (EVs) around the globe. Modern electric propulsion systems have seen considerable improvements in terms of their efficiency, durability, and performance as a result of recent advancements in battery technology, power electronics, and sophisticated control algorithms [1]. Because it has a direct impact on charging efficiency, battery longevity, driving range, and overall vehicle performance, the battery charging system is one of the most important components of an electric vehicle (EV) [2]. When it comes to regulating the charging of their batteries, conventional electric vehicles often make use of a specialized onboard charger that is comprised of various power conversion stages. Despite the fact that this method offers adequate charging performance, it results in a rise in the number of converters, the complexity of the hardware, the weight of the system, and the cost of production, while simultaneously lowering the total power density [3]. For the purpose of overcoming these limits, integrated onboard charging (IOC) technology has emerged as an appealing alternative. This technology makes use of the traction inverter and motor windings that are already there in order to charge the batteries. With this integrated design, hardware utilization is improved, converter redundancy is reduced, installation space is minimized, and system efficiency is increased without the need for an extra onboard charger [4]. As a result of its high efficiency, small size, high torque-to-weight ratio, broad speed operating range, and maintenance-free operation, the Brushless DC (BLDC) motor has emerged as one of the most popular options for electric vehicle (EV) propulsion among the numerous electric traction motors. Because it does not have brushes or commutators, the brushless direct current (BLDC) motor is particularly ideal for electric vehicle applications that need a rapid dynamic response and improved driving performance [5]. This is because the lack of these components increases dependability and minimizes mechanical losses. Nevertheless, the dynamic properties of a brushless direct current (BLDC) motor are highly dependent on the efficiency of the speed control approach that it employs. When functioning in steady-state settings, conventional proportional-integral (PI) controllers provide good performance. However, when working in nonlinear situations and with parameter fluctuations, these controllers suffer from overshoot, sluggish transient response, torque ripple, and lower resilience [6]. For electric vehicle propulsion systems, intelligent control strategies have been the subject of much research in order to solve these restrictions. The Fuzzy Logic Controller (FLC) is one of these controllers that has garnered a lot of interest due to the fact that it does not need a precise mathematical model and is able to efficiently deal with nonlinearities, uncertainties, and external disturbances [7]. When compared to conventional PI controllers, the FLC generates adaptive control actions that improve speed regulation, reduce settling time, suppress torque ripple, and enhance overall system robustness [8]. These actions are generated by processing the speed error and change in speed error through fuzzification, inference, and defuzzification. As a consequence of this, fuzzy logic control has been effectively used in applications that need high dynamic performance, such as motor drives, renewable energy systems, and electric vehicle applications [9], [10]. In order to be successful, integrated electric vehicle charging systems need to have excellent synchronization between charging and drive modes. When it is being charged, the traction inverter functions as an AC–DC converter; however, when it is being used for propulsion, it is providing power to the BLDC motor. That is why it is vital to have an intelligent control strategy in order to guarantee a smooth transition between these different modes of operation without the need for further hardware reconfiguration [11]. Additionally, bidirectional DC–DC buck–boost converters are used extensively due to the fact that they provide efficient battery charging, the potential to flow power in both directions, stable DC-link voltage management, and support for regenerative braking operation [12]. Recent research has concentrated on strengthening overall system dependability by using innovative converter topologies and intelligent control algorithms [13], [14]. This study has also focused on improving charging efficiency, lowering converter losses, and eliminating harmonic distortion. Many of the currently available studies concentrate largely on charging converter topologies or battery management, but they do not address the dynamic performance of the propulsion motor in a thorough manner. This is despite the fact that significant development has been made in the field of integrated electric vehicle charging technology. In a similar vein, a number of research are conducted on BLDC motor control that assess speed regulation separately without taking into consideration integrated charging operation 15. In addition, traditional PI-controlled BLDC drives often face a decline in performance when subjected to fast acceleration and deceleration, load disturbances, and fluctuations in battery voltage. This has led to the development of intelligent fuzzy logic-based control techniques [16], [17]. The employment of the existing inverter and motor windings during the process of battery charging results in a considerable reduction in hardware redundancy, manufacturing cost, converter count, and installation area, while simultaneously enhancing converter utilization and overall energy efficiency [18]. Nevertheless, high-performance integrated charging systems still need excellent DC-link voltage regulation, clever switching techniques, coordinated charging management, and dependable motor operation under transient situations [19]. The ability of fuzzy logic control to make decisions in an adaptive and rule-based manner makes it a promising solution for the development of future electric vehicle propulsion systems [20–22]. Fuzzy logic control offers improved speed regulation, disturbance rejection, reduced current ripple, and enhanced electromagnetic torque characteristics. This study offers a BLDC motor drive that is based on a Fuzzy Logic Controller and is combined with a single-phase electric car charging system. This work was motivated by the issues that have been presented. The design that has been presented makes use of a bidirectional DC–DC buck–boost converter, a common DC-link capacitor, voltage source inverters, and a BLDC motor in order to accomplish both propulsion and battery charging via the utilization of shared power electronic hardware [23–25]. The fuzzy logic controller is responsible for continually regulating the speed of the motor in accordance with the speed error and the change in speed error. This results in a better transient response, decreased torque ripple, increased speed tracking accuracy, and superior disturbance rejection [26], [28]. In the MATLAB/Simulink environment, the proposed system is modeled and verified under a variety of different operating situations. The results of the simulation showed that the charging operation was stable, that the performance of the BLDC motor was improved, that the steady-state error was decreased, and that the overall system efficiency was increased. This confirmed that the integrated electric vehicle charging design that was presented was successful.

Main Contributions of This Work

The main contributions of this paper are summarized as follows:

1. A novel integrated EV charging and propulsion system is proposed using a bridgeless boost PFC converter, bidirectional DC–DC buck–boost converter, common DC-link, and dual BLDC motor drive to improve system efficiency while reducing system complexity.
2. A Fuzzy Logic Controller (FLC) is designed for BLDC motor speed control to achieve improved speed regulation, reduced torque ripple, and enhanced dynamic performance compared with the conventional PI controller.
3. An efficient charging and energy management strategy is developed to provide near-unity power factor, low input current THD, stable DC-link voltage, and reliable battery charging during different operating modes.
4. The proposed system is validated in MATLAB/Simulink, demonstrating improved charging performance, enhanced motor characteristics, and higher overall efficiency for integrated electric vehicle applications.

II. SYSTEM CONFIGURATION

The power train architecture, shown in Fig. 1, comprises two traction motors, each mounted on the rear and front axle with an integrated power converter and battery pack. The proposed integrated electric vehicle (EV) charging and propulsion system is composed of a single-phase AC grid, a bridgeless boost power factor correction (PFC) totem-pole converter, a bidirectional DC–DC buck–boost converter, a common DC-link capacitor, dual three-phase voltage source inverters

(VSIs), and dual BLDC motors, as illustrated in Figs. 2 and 3. The system is designed to perform both battery charging and vehicle propulsion using a common power conversion platform, thereby reducing converter count, hardware complexity, and overall system cost. During the charging mode, the single-phase AC supply is connected through the SAE J1772 connector to the integrated charging circuit. The bridgeless boost PFC converter converts the AC input into a regulated DC voltage while achieving near-unity power factor and low input current harmonic distortion. The bidirectional DC–DC buck–boost converter regulates the battery charging current and maintains a constant DC-link voltage to ensure safe and efficient charging. During the driving mode, the EV battery supplies power to the DC-link through the bidirectional DC–DC converter. The regulated DC-link voltage is applied to the dual three-phase VSIs, which drive the dual BLDC motors to provide vehicle propulsion. A Fuzzy Logic Controller (FLC) generates the inverter switching signals based on the speed error and change in speed error, resulting in improved speed regulation, reduced torque ripple, faster transient response, and enhanced overall system efficiency compared with the conventional PI controller.

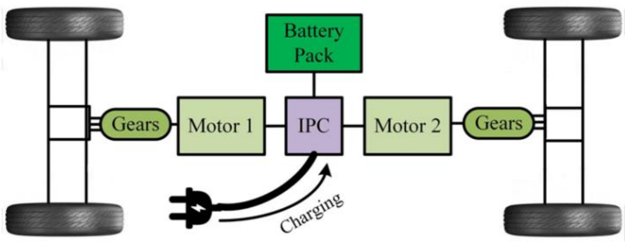

Fig. 1. Overall architecture of the integrated EV charging and propulsion system.

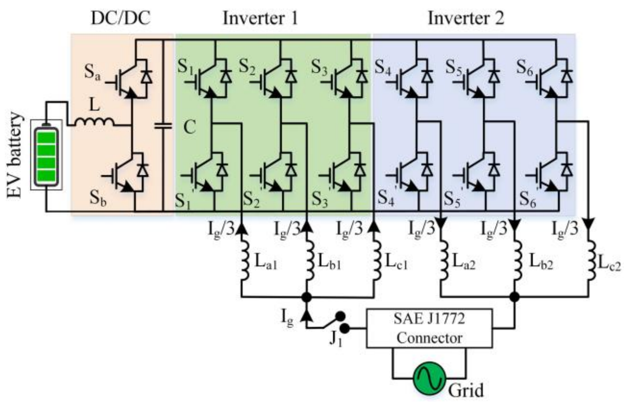

Fig. 2. Integrated EV charging system using dual traction inverters and bidirectional DC–DC converter.

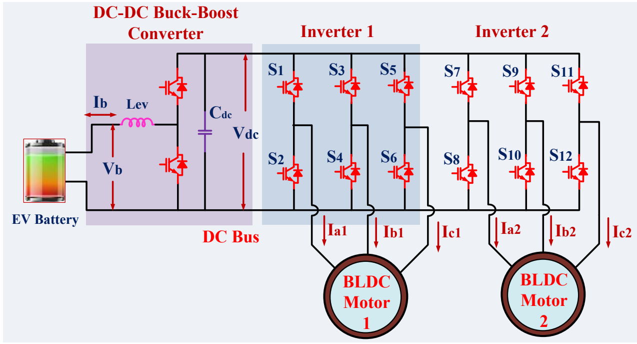

Fig. 3. Proposed dual BLDC motor drive with bidirectional DC–DC buck–boost converter.

III. CONTROL STRATEGY OF THE BRIDGELESS BOOST PFC TOTEM-POLE CONVERTER

The bridgeless boost power factor correction (PFC) totem-pole converter is employed to convert the single-phase AC grid voltage into a regulated DC-link voltage while maintaining near-unity power factor and low input current harmonic distortion as shown in Fig.4. The converter operates under continuous conduction mode (CCM) and consists of an outer voltage control loop and an inner current control loop. The outer voltage loop regulates the DC-link voltage, whereas the inner current loop shapes the input current to follow the grid voltage.

The instantaneous input voltage is expressed as

$$v_g(t) = V_m \sin(\omega t) \qquad (1)$$

Where

- Vm is the peak grid voltage,
- ω=2πf.

The reference input current is generated as

$$i_g^*(t) = K_v v_g(t) \qquad (2)$$

where

- Kv is obtained from the outer voltage controller.

A. Outer Voltage Control Loop

The DC-link voltage error is

$$e_v(t) = V_{dc}^* - V_{dc} \qquad (3)$$

The PI controller produces the current reference magnitude

$$I_m = K_p e_v + K_i \int e_v \, dt \qquad (4)$$

Hence,

$$i_g^* = I_m \frac{v_g}{Vg} \qquad (5)$$

which forces the input current to be sinusoidal and in phase with the grid voltage.

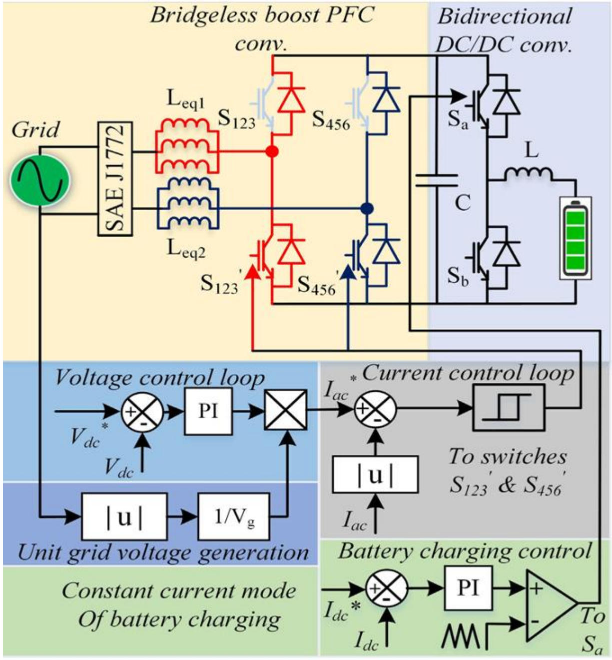

Fig. 4. Configuration of the bridgeless boost PFC and bidirectional DC–DC converter for the integrated EV battery charging system

B. Inner Current Control Loop

The current tracking error is

$$e_i = i_g^* - ig \tag{6}$$

The controller generates the PWM duty ratio

$$d = K_{pc} e_i + K_{ic} \int e_i \, dt \tag{7}$$

The generated PWM signals are applied to switches S123 and S456 according to the polarity of the grid voltage.

C. Battery Charging Controller

The charging current is regulated in constant-current mode.

The battery current error is

$$e_b = I_{dc}^* - I_{dc} \tag{8}$$

The PI controller determines the duty ratio of the bidirectional DC–DC converter

$$d_b = K_{pb} e_b + K_{ib} \int e_b dt \tag{9}$$

which guarantees constant-current battery charging.

IV. BIDIRECTIONAL DC–DC BUCK–BOOST CONVERTER

The bidirectional DC–DC buck–boost converter serves as the energy management interface between the EV battery and the DC-link. It enables bidirectional power transfer by operating in buck mode during battery charging and boost mode during vehicle propulsion. The converter regulates the battery charging current, maintains a constant DC-link voltage, and supports efficient energy transfer with reduced switching losses. The converter consists of two complementary power switches Sa and Sb, an inductor Lev, and a DC-link capacitor Cdc, as shown in Fig. 5.

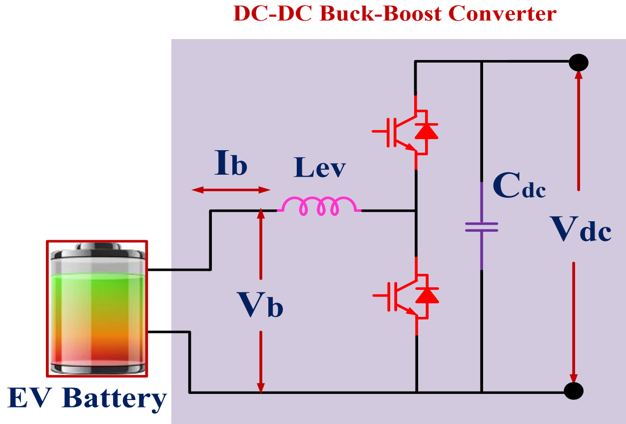

Fig. 5. Bidirectional DC–DC converter for DC-link voltage regulation and battery charging

A. Boost Mode (Vehicle Driving)

During the driving operation, the battery supplies power to the traction inverter through the DC–DC converter. In this mode, the converter operates as a boost converter, where the battery voltage Vb is stepped up to the required DC-link voltage Vdc.

When switch Sa is ON and Sb is OFF, the inductor stores energy from the battery. Applying Kirchhoff's Voltage Law (KVL),

$$\frac{di_b}{dt} = \frac{V_b}{L_{ev}} \tag{10}$$

During the OFF interval, the stored energy is transferred to the DC-link capacitor through the diode, giving

$$\frac{di_b}{dt} = \frac{V_b - V_{dc}}{L_{ev}} \tag{11}$$

The DC-link capacitor voltage is governed by

$$C_{dc} \frac{dV_{dc}}{dt} = i_b - \frac{V_{dc}}{R} \tag{12}$$

where

- ib = battery current,
- Vb = battery voltage,
- V_{dc} = DC-link voltage,
- R = equivalent DC-link load resistance.

B. Buck Mode (Battery Charging)

During charging, power flows from the DC-link to the battery. The converter operates as a buck converter, where the DC-link voltage is stepped down to the battery charging voltage.

When switch Sb is ON,

$$\frac{di_b}{dt} = \frac{V_{dc} - V_b}{L_{ev}} \tag{13}$$

During the OFF interval,

$$\frac{di_b}{dt} = -\frac{V_b}{L_{ev}} \tag{14}$$

The charging current is regulated by adjusting the duty ratio to maintain constant-current charging.

C. Voltage Conversion Ratio

Boost Mode

The steady-state voltage gain is

$$V_{dc} = \frac{V_b}{1-D} \quad (15)$$

Where

D is the duty cycle.

Buck Mode

The voltage conversion ratio becomes

$$V_b = DV_{dc} \quad (16)$$

The bidirectional DC–DC buck–boost converter operates as the energy management stage of the proposed EV system. During charging, it functions in buck mode to regulate the battery charging current while maintaining safe charging conditions. During vehicle propulsion, it operates in boost mode to elevate the battery voltage to the required DC-link level for the dual voltage source inverters. By controlling the duty ratio of the active switches, the converter ensures stable DC-link voltage, efficient bidirectional power transfer, and reliable operation under varying load and battery conditions. This coordinated operation enhances overall system efficiency, battery utilization, and dynamic performance of the integrated EV charging and propulsion system.

V. BLDC MOTOR DRIVE DESIGN AND OPERATING PRINCIPLE

The proposed electric vehicle propulsion system employs a three-phase Brushless DC (BLDC) motor supplied by a Voltage Source Inverter (VSI). As illustrated in Fig. 6, the DC-link voltage Vdc obtained from the bidirectional DC–DC converter is applied to the three-phase VSI. The inverter consists of six power semiconductor switches (S1–S6), which are controlled according to the rotor position information obtained from three Hall-effect sensors (H1,H2,H3). The Hall sensor outputs are processed by the electronic commutation unit to generate the appropriate switching sequence for the inverter. Simultaneously, the fuzzy logic controller regulates the PWM duty ratio to control the inverter output voltage and thereby maintain the desired motor speed.

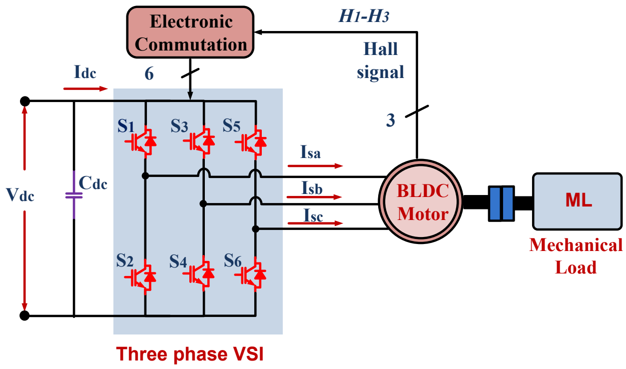

Fig. 6. Electronic commutation circuit for the proposed BLDC motor drive.

A. BLDC Motor Mathematical Model

Considering a balanced three-phase BLDC motor, the stator voltage equations are

$$V_a = Ri_a + L\frac{di_a}{dt} + e_a \quad (17)$$

$$V_b = Ri_b + L\frac{di_b}{dt} + e_b \quad (18)$$

$$V_c = Ri_c + L\frac{di_c}{dt} + e_C \quad (19)$$

where

- Va,Vb,Vc are the phase voltages,
- ia,ib,ic are the phase currents,
- R is the phase resistance,
- L is the phase inductance,
- ea,eb,ec are the trapezoidal back-EMFs.

The back-EMFs are expressed as

$$e_a = K_e f_a(\theta_e)\omega_r \quad (20)$$

$$e_b = K_e f_b(\theta_e)\omega_r \quad (21)$$

$$e_c = K_e f_c(\theta_e)\omega_r \quad (22)$$

where

- Ke is the back-EMF constant,
- ωr is the rotor speed,
- θe is the electrical rotor position,
- fa(θe), fb(θe), and fc(θe) are the trapezoidal back-EMF functions.

B. Electromagnetic Torque

The developed electromagnetic torque is

$$Te = \frac{e_a i_a + e_b i_b + e_c i_c}{\omega_r} \quad (23)$$

For an ideal BLDC motor,

$$T_e = K_t I \quad (24)$$

where

- Kt is the torque constant,
- I is the effective phase current.

C. Mechanical Dynamics

The rotor dynamics are governed by

$$J\frac{d\omega_r}{dt} = T_e - T_L - B\omega_r \quad (25)$$

where

- J is the rotor inertia,
- B is the viscous friction coefficient,
- TL is the mechanical load torque.

The rotor position is

$$\frac{d\theta_r}{dt} = \omega_r \qquad (26)$$

VI. FUZZY LOGIC CONTROLLER DESIGN

The proposed Brushless DC (BLDC) motor drive employs a Mamdani-type Fuzzy Logic Controller (FLC) for speed regulation. The controller utilizes the speed error and change in speed error as input variables to generate the control signal for pulse-width modulation (PWM). The generated PWM signals are combined with the rotor position information obtained from the Hall-effect sensors to produce the switching sequence of the three-phase voltage source inverter (VSI) as shown in Fig.7. Consequently, the proposed controller ensures accurate speed regulation, smooth electronic commutation, and reduced electromagnetic torque ripple under varying operating conditions.

A. Speed Control Model

The speed error is calculated as

$$e(k) = \omega_r^*(k) - \omega_r(k) \qquad (27)$$

where

- ωr∗ = reference speed,
- ωr = measured speed.

The change in speed error is

$$\Delta e(k) = e(k) - e(k-1) \qquad (28)$$

The controller input vector becomes

$$X(k) = \begin{bmatrix} e(k) \\ \Delta e(k) \end{bmatrix} \qquad (29)$$

The fuzzy controller generates

$$u(k) = F[e(k), \Delta e(k)] \qquad (30)$$

where u(k) is the controller output

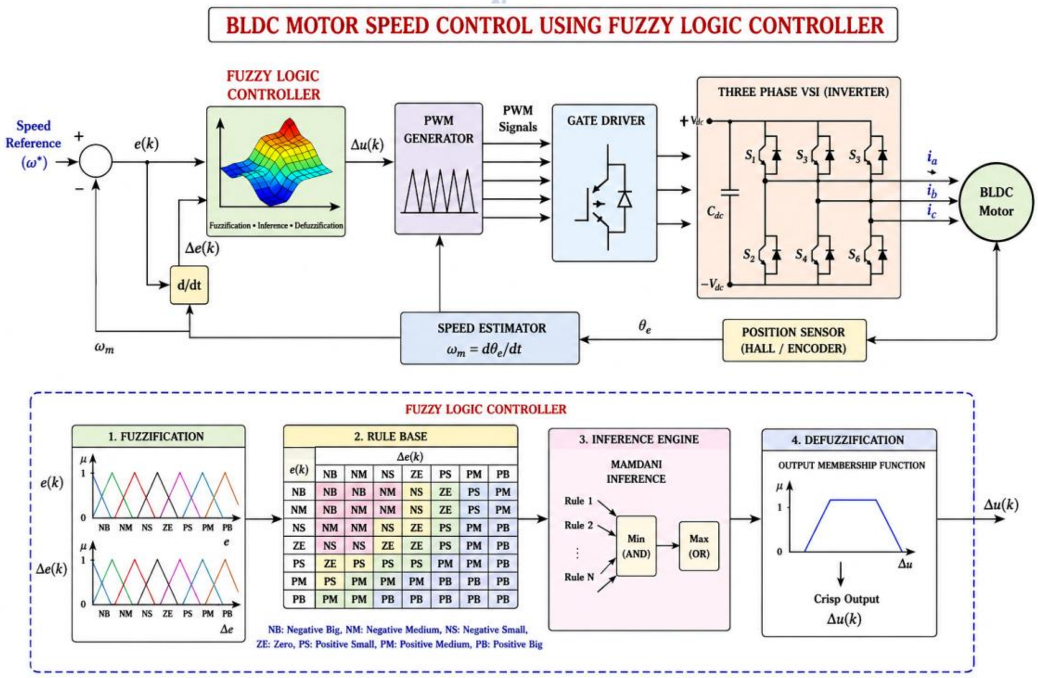

Fig. 7. Proposed BLDC motor speed control using a fuzzy logic controller

B. Fuzzification

The controller employs seven linguistic variables {NB,NM,NS,ZE,PS,PM,PB}

The triangular membership function is

$$\mu(x) = \begin{cases} 0, & x \le a \\ \frac{x-a}{b-a}, & a < x \le b \\ \frac{c-x}{c-b}, & b < x < c \\ 0, & x \ge c \end{cases} \qquad (31)$$

where a, b, and c define the triangular membership limits.

C. Fuzzy Rule Base

The controller consists of 25 IF–THEN rules.

A general rule is

IF e is A_i AND Δ_e is B_j THEN u is C_{ij} (32)

where

- A_i = speed error fuzzy set,
- B_j = change in error fuzzy set,
- C_{ij} = output fuzzy set.

D. Mamdani Inference Mechanism

The firing strength of each rule is determined using the minimum operator,

$\alpha_i = \min[\mu_e, \mu\Delta_e]$ (33)

The aggregated output is

$\mu_0 = \max(\alpha_1, \alpha_2 \ldots, \alpha_{25})$ (34)

E. Defuzzification

The centroid method converts the fuzzy output into a crisp control signal

$u = \frac{\Sigma \mu_i z_i}{\Sigma \mu_i}$ (35)

where

- zi denotes the centroid of the output membership function.

F. PWM Generation

The controller output regulates the PWM duty ratio,

$D(k) = D(k-1) + u(k)$ (36)

The PWM signal is generated by comparing the controller output with a high-frequency triangular carrier,

$PWM = \begin{cases} 1, & u > V_{tri} \\ 0, & u < V_{tri} \end{cases}$ (37)

where

- V_{tri} is the carrier signal.

G. Hall Sensor-Based Electronic Commutation

The proposed BLDC drive employs three Hall-effect sensors mounted 120° electrical apart to detect the rotor position. The Hall sensors generate three digital signals

$H = (H_A, H_B, H_C)$ (38)

Where

$H_A, H_B, H_C \in \{0,1\}$ (39)

The Hall sensor outputs determine the commutation sequence of the three-phase VSI. Based on the detected rotor position, two inverter switches are turned ON while the remaining phase is left floating, ensuring continuous electromagnetic torque production.

The Hall sensor decoding function is expressed as

$\theta_r = f(H_A, H_B, H_C)$ (40)

where

- θr is the rotor electrical position.

The inverter switching function is

$S = f(\theta_r, PWM)$ (41)

where

- S=[S1,S2,S3,S4,S5,S6] denotes the gate signals of the VSI switches.

Table-1Hall Sensor Commutation

Hall Sensors	Rotor Position	Active Switches	Conducting Phases
101	0°–60°	S1–S4	A+, B−
100	60°–120°	S1–S6	A+, C−
110	120°–180°	S3–S6	B+, C−
010	180°–240°	S3–S2	B+, A−
011	240°–300°	S5–S2	C+, A−
001	300°–360°	S5–S4	C+, B−

H. Controller Operation

The reference speed is continuously compared with the measured motor speed to generate the speed error and change in speed error. These variables are processed through the fuzzification, inference, and defuzzification stages to obtain the PWM control signal. Simultaneously, the Hall sensors provide real-time rotor position information for electronic commutation. The PWM signal and Hall sensor outputs are combined to generate the switching pulses for the three-phase voltage source inverter. This coordinated control strategy ensures accurate speed tracking, smooth commutation, reduced torque ripple, and improved dynamic response under varying load conditions.

VII. SIMULATION RESULTS AND DISCUSSION

A. EV Charging Mode Performance

The proposed EV charging system was modeled and simulated in MATLAB/Simulink to evaluate the performance of the bridgeless boost PFC converter and bidirectional DC–DC converter during grid-to-vehicle (G2V) charging. The performance was assessed in terms of input voltage and current synchronization, power factor correction, and DC-link voltage regulation.

a) Grid Voltage, Power Factor, and DC-Link Voltage Performance

The steady-state performance of the proposed Grid-to-Vehicle (G2V) charging system is presented in Fig. 8. As shown in Fig. 8(a), the grid voltage and input current exhibit sinusoidal waveforms with steady-state amplitudes of approximately ±230 V and ±100 A, respectively. The input current remains synchronized with the grid voltage, indicating effective current shaping by the bridgeless boost power factor correction converter and ensuring high-quality power transfer from the utility grid to the EV battery with negligible phase displacement. The power factor response shown in Fig. 8(b) settles at approximately 1.0, confirming near-unity power factor operation and effective reactive power compensation under steady-state charging conditions. Furthermore, the DC-link voltage illustrated in Fig. 8(c) is regulated at approximately 500 V with only a small steady-state voltage ripple, providing a stable DC source for the downstream bidirectional DC–DC converter and EV battery charging. The steady-state results demonstrate that the proposed G2V charging system achieves sinusoidal grid voltage and current, unity power factor, and stable DC-link voltage regulation, thereby ensuring efficient, reliable, and high-performance battery charging.

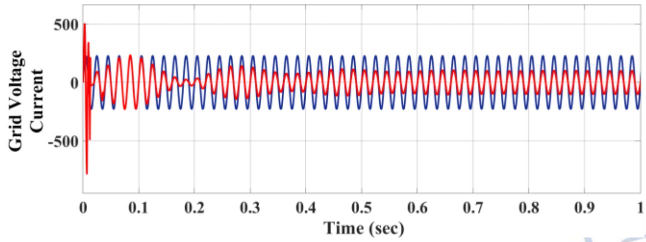

(a)

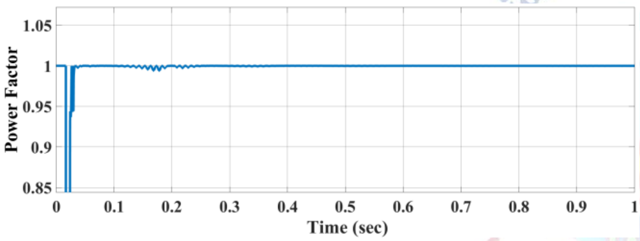

(b)

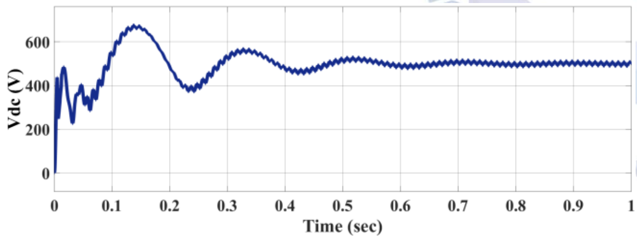

(c)

Fig. 8. Performance of the proposed Grid-to-Vehicle (G2V) charging system: (a) Grid voltage and input current, (b) Power factor response, and (c) DC-link voltage response.

b) EV Battery Charging Performance Analysis

The EV battery charging performance of the proposed Grid-to-Vehicle (G2V) charging system under steady-state conditions is presented in Fig. 9. As shown in Fig. 9(a), the EV battery voltage is successfully regulated at approximately 325 V, demonstrating stable voltage control throughout the charging process. The corresponding charging current in Fig. 9(b) settles at approximately −35 A, indicating a constant and controlled charging current supplied to the battery. The EV charging power shown in Fig. 9(c) reaches a steady-state value of approximately −12 kW, confirming continuous and efficient power transfer from the grid to the EV battery. Furthermore, the battery state of charge (SOC) illustrated in Fig. 9(d) increases gradually from approximately 79.320% to 79.323% during the simulation period, indicating continuous energy storage under stable charging conditions. The stable battery voltage, constant charging current, regulated charging power, and gradual increase in SOC demonstrate the effectiveness of the proposed G2V charging strategy in achieving reliable, efficient, and stable EV battery charging.

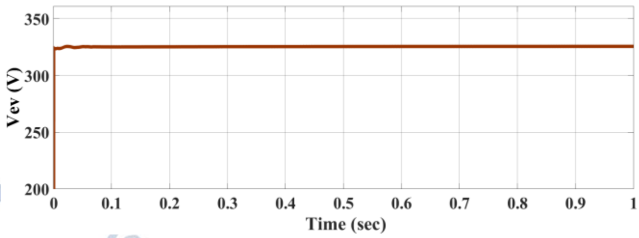

(a)

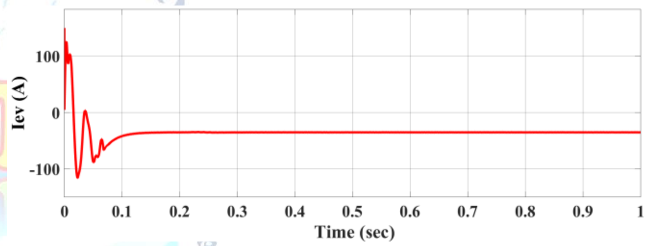

(b)

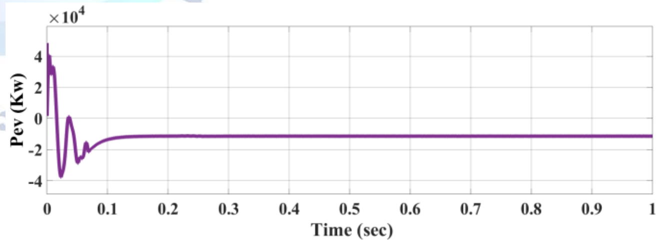

(c)

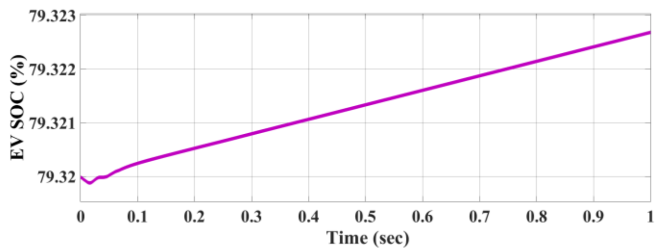

(d)

Fig. 10. EV battery charging performance of the proposed Grid-to-Vehicle (G2V) charging system: (a) EV battery voltage, (b) EV charging current, (c) EV charging power, and (d) EV battery state of charge (SOC).

B. EV Driving Mode Performance Analysis

The performance of the proposed EV driving system was evaluated under battery-powered operation, where the EV battery supplies energy to the dual BLDC motors through the bidirectional DC–DC buck–boost converter. During vehicle propulsion, the battery current controller regulates the battery discharge current, while the DC-link voltage controller maintains a constant DC-link voltage to ensure stable operation of both three-phase inverters. The corresponding simulation results are presented in Fig. 10. As shown in Fig. 10(a), the EV battery voltage is maintained at approximately 325 V, indicating stable battery operation during propulsion. The battery current shown in Fig. 10(b) settles to approximately 10 A after the initial transient, demonstrating effective regulation by the battery current controller and controlled energy delivery to the BLDC motors. The battery power illustrated in Fig. X(c) reaches a steady-state value of approximately 5 kW, confirming continuous power transfer from the battery to the propulsion system. The battery state of charge (SOC) shown in Fig. 10(d) gradually decreases from approximately 79.320% to 79.319%, representing the normal battery discharge during vehicle operation. Furthermore, the DC-link voltage presented in Fig. 10(e) is successfully regulated at approximately 500 V with only a small steady-state ripple, demonstrating the effectiveness of the DC-link voltage controller in maintaining a constant DC bus voltage despite variations in motor load demand. The coordinated operation of the bidirectional DC–DC converter, battery current controller, and DC-link voltage controller ensures stable battery discharge, regulated DC-link voltage, and reliable power delivery to both BLDC motor drives, thereby improving the dynamic performance and overall efficiency of the proposed EV propulsion system.

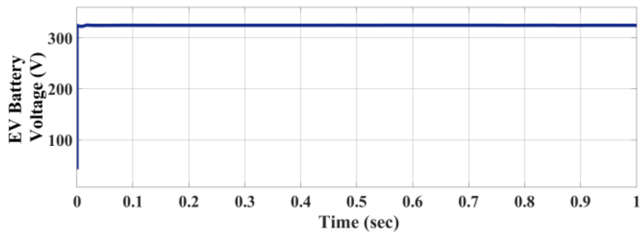

(a)

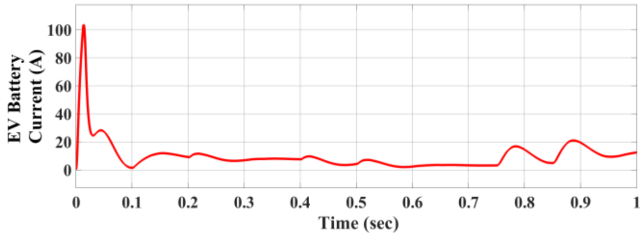

(b)

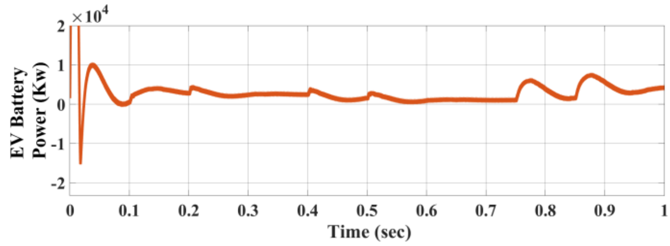

(c)

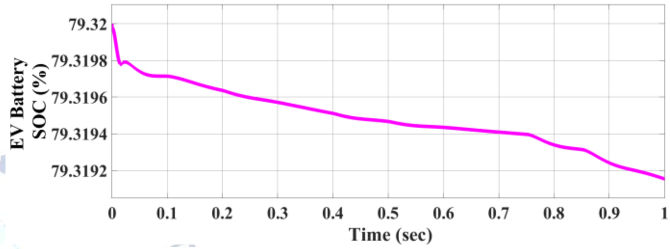

(d)

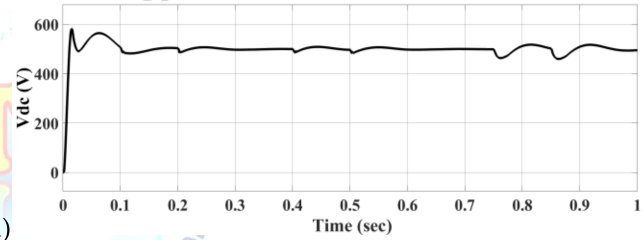

(e)

Fig. 10. Performance of the proposed EV driving mode: (a) EV battery voltage, (b) EV battery current, (c) EV battery power, (d) EV battery state of charge (SOC), and (e) DC-link voltage.

C. Performance Analysis of the Proposed Dual Inverter-Connected BLDC Motor Drive

The dynamic performance of the proposed dual inverter-connected BLDC motor drive was evaluated under different operating speeds and load conditions, and the corresponding simulation results are presented in Fig. 11. The bidirectional DC–DC buck–boost converter maintains a regulated DC-link voltage of approximately 500 V, while the two independent three-phase voltage source inverters supply power to BLDC Motor 1 and BLDC Motor 2. The fuzzy logic speed controller generates the appropriate PWM signals for both inverters to ensure accurate speed tracking and stable motor operation. As shown in Fig. 11(a), the phase current of BLDC Motor 1 reaches a steady-state amplitude of approximately ±10 A during normal operation. During speed transitions, the current briefly increases to nearly ±45 A to satisfy the transient torque demand before returning to its steady-state value. The corresponding speed response in Fig. 11(b) demonstrates that Motor 1 accurately follows the reference speed commands of 3000 rpm, 1500 rpm, 500 rpm, and again 3000 rpm, exhibiting fast dynamic response with negligible steady-state error. The electromagnetic torque shown in Fig. 11(c) settles at approximately 5 N·m during steady-state operation, while transient torque peaks of nearly ±40 N·m are observed during rapid acceleration and deceleration, indicating effective torque control. Similarly, the performance of BLDC Motor 2 is illustrated in Fig. 11(d)–(f). The motor phase current stabilizes at approximately ±10 A, while transient peaks of about ±45 A occur during changes in the reference speed. The speed response in Fig. 11(e) accurately tracks the commanded speeds of 3000 rpm, 1500 rpm, 500 rpm, and 3000 rpm, confirming the independent speed regulation capability of the second inverter. The corresponding electromagnetic torque shown in Fig. 11(f) settles at approximately 5 N·m during steady-state operation and produces transient peaks of approximately ±40 N·m during speed transitions, thereby providing sufficient accelerating and braking torque. The simulation results confirm that the proposed dual inverter topology enables independent control of both BLDC motors while maintaining excellent speed tracking, regulated motor current, stable electromagnetic torque, and fast transient response. The coordinated operation of the bidirectional DC–DC converter, dual voltage source inverters, Hall sensor-based electronic commutation, and fuzzy logic controller ensures reliable and efficient propulsion performance suitable for electric vehicle applications.

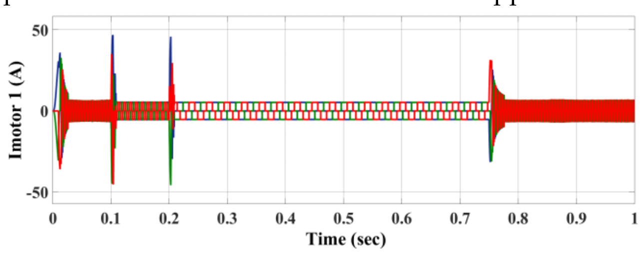

(a)

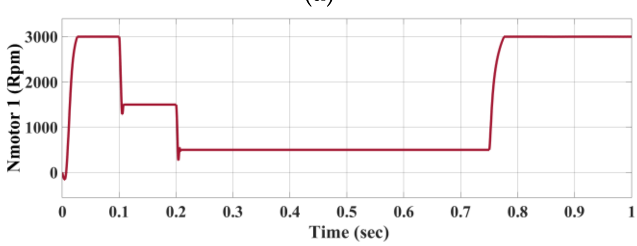

(b)

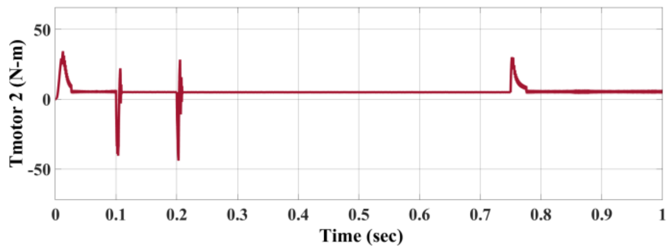

(c)

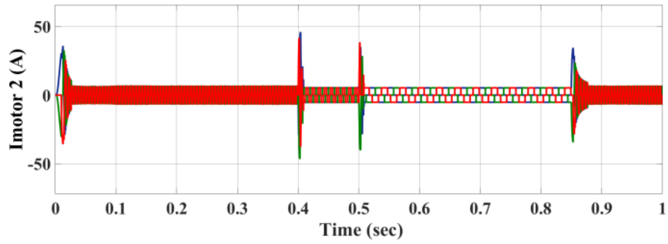

(d)

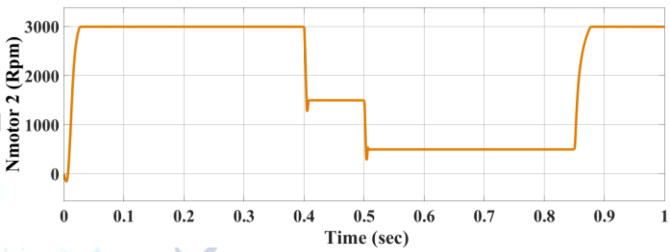

(e)

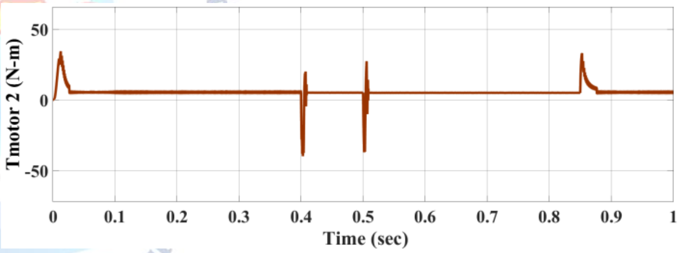

(f)

Fig. 11. Dynamic performance of the proposed dual inverter-connected BLDC motor drive: (a) phase current of BLDC Motor 1, (b) speed response of BLDC Motor 1, (c) electromagnetic torque of BLDC Motor 1, (d) phase current of BLDC Motor 2, (e) speed response of BLDC Motor 2, and (f) electromagnetic torque of BLDC Motor 2.

D. Comparative Performance Analysis of PI and Fuzzy Logic Controllers

The performance of the proposed Fuzzy Logic Controller (FLC) was compared with that of the conventional PI controller under identical operating conditions, and the results are presented in Fig. 12. As shown in Fig. 12(a) and Fig. 12(c), the FLC enables both BLDC motors to accurately follow the reference speed commands of 3000 rpm, 1500 rpm, 500 rpm, and 3000 rpm with negligible overshoot and faster settling time. In contrast, the PI controller exhibits a significant speed overshoot of approximately 4200 rpm during acceleration and requires a longer time to reach steady-state operation. The corresponding electromagnetic torque responses shown in Fig. 12(b) and Fig. 12(d) indicate that both controllers produce transient torque peaks of approximately ±50 N·m during speed changes. However, the FLC rapidly suppresses the torque oscillations and settles to the steady-state torque of approximately 5 N·m, whereas the PI controller exhibits comparatively larger oscillations and slower damping. These results demonstrate that the proposed FLC provides superior speed tracking performance, reduced overshoot, lower torque ripple, and improved dynamic response compared with the conventional PI controller, thereby enhancing the overall performance of the dual inverter-connected BLDC motor drive for electric vehicle propulsion.

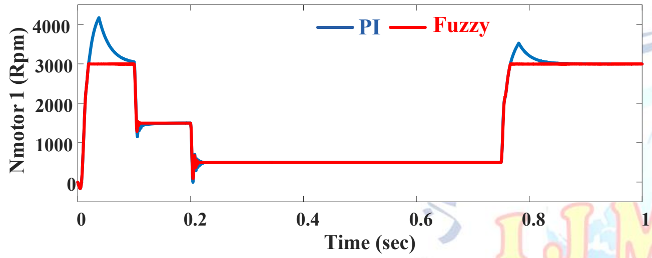

(a)

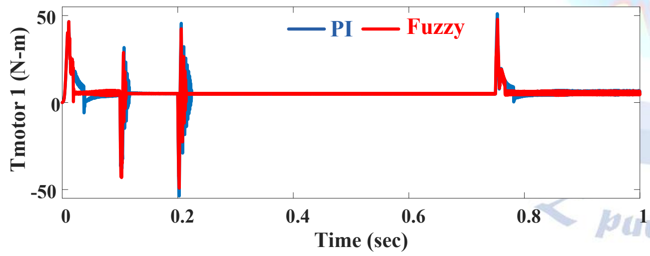

(b)

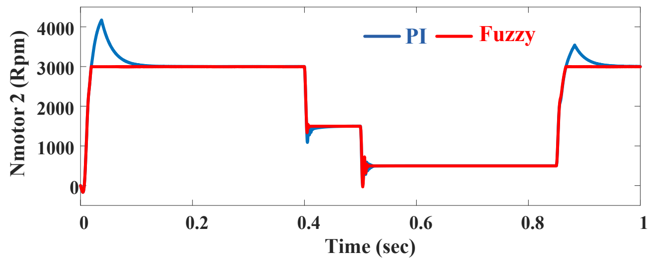

(c)

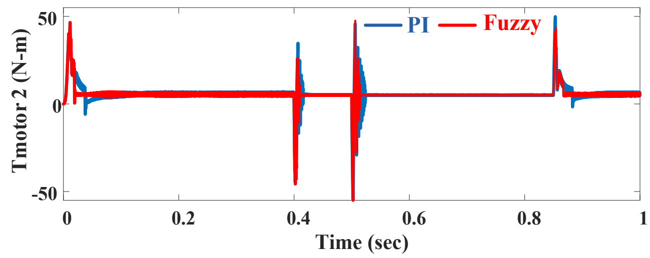

(d)

Fig. 12. Comparison of PI and fuzzy logic controllers: (a) Speed response of BLDC Motor 1, (b) Electromagnetic torque of BLDC Motor 1, (c) Speed response of BLDC Motor 2, and (d) Electromagnetic torque of BLDC Motor 2.

VIII. CONCLUSION

This paper presented the design and performance analysis of a Fuzzy Logic Controller (FLC)-based integrated electric vehicle charging and propulsion system using dual BLDC motors. The proposed system employs a bridgeless boost power factor correction converter, a bidirectional DC–DC buck–boost converter, and dual three-phase voltage source inverters to achieve efficient battery charging and reliable vehicle propulsion through a common DC-link architecture. During the charging mode, the proposed control strategy ensured improved input power quality, stable DC-link voltage regulation, and effective battery charging. During the driving mode, the bidirectional converter and dual inverter configuration provided reliable power distribution to the BLDC motors, while the FLC achieved accurate speed regulation and smooth torque control under varying operating conditions. Simulation results validated the effectiveness of the proposed system in charging and propulsion modes, demonstrating stable system operation, reliable energy management, and improved dynamic performance. Furthermore, comparative analysis confirmed that the proposed FLC outperformed the conventional PI controller by providing faster dynamic response, enhanced speed tracking capability, reduced overshoot, and lower torque ripple. Overall, the proposed integrated charging and propulsion architecture offers a compact, efficient, and reliable solution for electric vehicle applications and provides a promising control strategy for future high-performance EV drive systems.

Conflict of interest statement

Authors declare that they do not have any conflict of interest.

REFERENCES

[1] A. Khaligh and S. Dusmez, "Comprehensive Topological Analysis of Conductive and Inductive Charging Solutions for Plug-In Electric Vehicles," IEEE Transactions on Vehicular Technology, vol. 61, no. 8, pp. 3475–3489, Oct. 2012.

[2] F. Nasr Esfahani, A. Darwish, M. Ma, and P. Twigg, "Non-Integrated and Integrated On-Board Battery Chargers

(iOBCs) for Electric Vehicles (EVs): A Critical Review," Energies, vol. 17, no. 10, 2024.
[3] A. R. Dar et al., "On-Board Chargers for Electric Vehicles: A Comprehensive Performance and Efficiency Review," Energies, vol. 17, 2024.
[4] M. Mehmood et al., "Sliding Mode Control of Single-Phase Interleaved Totem-Pole PFC for Electric Vehicle Onboard Chargers," IEEE Transactions on Vehicular Technology, vol. 67, no. 9, pp. 8100–8109, Sept. 2018.
[5] Lin, Chang-Hua, Hom-Wei Liu, and Chien-Ming Wang. "Design and implementation of a bi-directional power converter for electric bike with charging feature." Industrial Electronics and Applications (ICIEA), 2010 the 5th IEEE Conference on. IEEE, 2010.
[6] Rajan Kumar, Bhim Singh, "Buck-Boost Converter Fed BLDC Motor Drive for Solar PV Array Based Water Pumping" IEEE International Conference on Power Electronics, Drives and Energy Systems(PEDES), P.P 1-6, Dec 2014.
[7] Bhajana, V. V., and Pavel Drabek. "A novel ZCS bidirectional buck-boost DC-DC converters for energy storage applications." Industrial Technology (ICIT), 2015 IEEE International Conference on. IEEE, 2015.
[8] Atul Kumar, Dr. Prerna Gaur "Bidirectional DC/DC Converter for Hybrid Electric Vehicle" IEEE Transactions on Advances in Computing, Communications and Informatics (ICACCI),P.P 839-843,sep 2014.
[9] Kumar, V. Vijaya, V. Udayakumar, and J. Muruganandham. "Speed control of BLDC motor for four quadrant operation without loss of power."Computation of Power, Energy Information and Commuincation (ICCPEIC), 2015 International Conference on. IEEE, 2015.
[10] Awaze, Sneha K. "Four quadrant operation of BLDC motor in MATLAB/SIMULINK." Computational Intelligence and Communication Networks (CICN), 2013 5th International Conference on. IEEE, 2013.
[11] Vinatha, U, Pola, S. ; Vittal, K.P. "simulation of four quadrant operation & speed control of BLDC motor on MATLAB/SIMULINK"TENCON, P.P 1-6,2008
[12] Joice, C. Sheeba, and P. Nivedhitha. "Simulation of speed control of brushless dc motor, with fuzzy logic controller." International Journal of Electrical, Electronics and Data Communication, ISSN: 2320-2084.
[13] Kamal, Md Mustafa, Lini Mathew, and S. Chatterji. "Speed control of Brushless DC Motor using fuzzy based controllers." Electrical, Electronics and Computer Science (SCEECS), 2014 IEEE Students' Conference on. IEEE, 2014.
[14] Sreekala, P., and A. Sivasubramanian. "Speed control of brushless DC motor with PI and fuzzy logic controller using resonantpole inverter."Innovative Smart Grid TechnologiesIndia (ISGT India), 2011 IEEE PES. IEEE, 2011.
[15] Sriram, J., and K. Sureshkumar. "Speed control of BLDC motor using fuzzy logic controller based on sensorless technique." Green Computing Communication and Electrical Engineering (ICGCCEE), 2014 International Conference on. IEEE, 2014.
[16] Blessy, M. S., and M. Murugan. "Modeling and controlling of BLDC motor based fuzzy logic." Information Communication and Embedded Systems (ICICES), 2014 International Conference on. IEEE, 2014.
[17] Donescu, V., Neacsu, D. O., & Griva, G. (1996, June). Design of fuzzy logic speed controller for brushless DC motor drives. In Industrial Electronics, 1996. ISIE'96., Proceedings of the IEEE International Symposium on (Vol. 1, pp. 404-408). IEEE.
[18] Siong, T. C., Ismail, B., Siraj, S. F., Mohammed, M. F., & Tajuddin, M. F. N. (2010, November). Implementation of Fuzzy Logic controller for permanent magnet brushless DC motor drives. In Power and Energy (PECon), 2010 IEEE International Conference on (pp. 462-467). IEEE.
[19] Blessy, M. S., & Murugan, M. (2014, February). Modeling and controlling of BLDC motor based fuzzy logic. In Information Communication and Embedded Systems (ICICES), 2014 International Conference on (pp. 1-6). IEEE.
[20] Joice, C. S., Paranjothi, S. R., & Kumar, J. S. (2011, December). Practical implementation of four quadrant operation of three phase Brushless DC motor using dsPIC. In Recent Advancements in Electrical, Electronics and Control Engineering (ICONRAEeCE), 2011 International Conference on (pp. 91-94). IEEE.
[21] Ganesh, C., et al. "A Non-Iterative controller design for a BLDC Drive system." Advances in Recent Technologies in Communication and Computing, 2009. ARTCom'09. International Conference on. IEEE, 2009.
[22] Gupta, Gaurav, and Prerna Gaur. "Fuzzy logic controlled-power factor corrected bridgeless buck boost converter-fed brushless DC motor drive."Computer, Communication and Control (IC4), 2015 International Conference on. IEEE, 2015.
[23] Awaze, Sneha K. "Four quadrant operation of BLDC motor in MATLAB/SIMULINK." Computational Intelligence and Communication Networks (CICN), 2013 5th International Conference on. IEEE, 2013.
[24] Kalavathi, M. Surya, and C. Subba Rami Reddy. "Performance evaluation of classical and fuzzy logic control techniques for brushless DC motor drive."Power Modulator and High Voltage Conference (IPMHVC), 2012 IEEE International. IEEE, 2012.
[25] Arulmozhiyal, R. "Design and implementation of fuzzy PID controller for BLDC motor using FPGA." Power Electronics, Drives and Energy Systems (PEDES), 2012 IEEE International Conference on. IEEE, 2012.
[26] Al-Jazaeri, A. O., et al. "Fuzzy Logic Control for energy saving in Autonomous Electric Vehicles." Electric Vehicle Conference (IEVC), 2014 IEEE International. IEEE, 2014.
[27] Shamseldin, Mohammed Abdelbar, and Adel A. El-Samahy. "Speed control of BLDC motor by using PID control and selftuning fuzzy PID controller."Research and Education in Mechatronics (REM), 2014 15th International Workshop on. IEEE, 2014.
[28] Krishnan, P. Hari, and M. Arjun. "Control of BLDC motor based on adaptive fuzzy logic PID controller." Green Computing Communication and Electrical Engineering (ICGCCEE), 2014 International Conference on. IEEE, 2014.